PHYSICS DESIGN OF APT LINAC WITH NORMAL CONDUCTING RF CAVITIES*

S. Nath, J. H. Billen, J. E. Stovall, H. Takeda, and L. M. Young
Los Alamos National Laboratory, MS H817, Los Alamos, NM 87545, USA

Abstract

The accelerator based production of tritium calls for a high-power, cw proton linac. Previous designs for such a linac use a radio-frequency quadrupole (RFQ), followed by a drift-tube linac (DTL) to an intermediate energy and a coupled-cavity linac (CCL) to the final energy. The Los Alamos design uses a high-energy (6.7-MeV) RFQ followed by the newly developed [1] coupled-cavity drift-tube linac (CCDTL) and a CCL. This design accommodates external electromagnetic quadrupole lenses which provide a strong uniform focusing lattice from the end of the RFQ to the end of the CCL.

The cell lengths in linacs of traditional design are typically graded as a function of the particle velocity. By making groups of cells symmetric in both the CCDTL and CCL, the cavity design as well as the mechanical design and fabrication is simplified without compromising the performance. At higher energies, there are some advantages of using superconducting rf cavities. Currently, such schemes are under vigorous study [2]. Here, we describe the linac design based on normal conducting cavities and present the simulation results.

Introduction

The linac for the production of tritium calls for 100 mA of cw proton beam to be delivered onto a production target. The main challenge in the design comes from the hands-on maintenance requirement of the entire linac by way of permissible beam loss along its length. Thus, elimination of known causes of beam-loss and control of transverse emittance growth (implying larger transverse spread of beam particles) are of utmost concern in the design of such a linac. In the room temperature design, we minimized the number of transitions between accelerating structures. In contrast to earlier designs [3], the only transition we have is between the RFQ and the CCDTL. In addition to eliminating all but one transition, we do not have a separate matching-section between the RFQ and the CCDTL. Instead, the transport properties in both the transverse and longitudinal motion are tailored to be continuous at the end of the RFQ and the beginning of the CCDTL, thus avoiding a discontinuity in the restoring forces experienced by the beam.

A schematic of the linac is shown in Fig. 1. It consists of an RFQ followed by a CCDTL and a CCL. The RFQ accelerates the beam from 75 keV to 6.7 MeV and the CCDTL takes the beam to 100 MeV. A CCL accelerates the beam to a final energy of 1.3 GeV.

* Work supported by the US Department of Energy.

RFQ Accelerator

The cw RFQ for the APT linac produces a 100-mA beam of protons with an output energy of 6.7 MeV. An engineering drawing of the RFQ is contained in Ref. 3. The conceptual design is described in complete detail elsewhere [3-4]. This is an 8-m long rf structure consisting of four 2-m-long segments that are resonantly coupled together. Each segment is a resonant structure assembled from two 1-m-long brazed sections.

The RFQ design uses an improved beam-dynamics code [5] that includes multipole field effects. It has been benchmarked successfully against other codes [6]. The transverse current limit is greater than 240 mA throughout the length of the structure. The longitudinal current limit exceeds 150 mA beyond the 1-MeV point. The peak surface field along the length of the vane-tips does not exceed 1.8 times the Kilpatrick limit.

In the high-energy part of the RFQ, we specially tailor the vane-tip modulation to increase the longitudinal focusing strength thereby reducing the phase width of the exit beam.

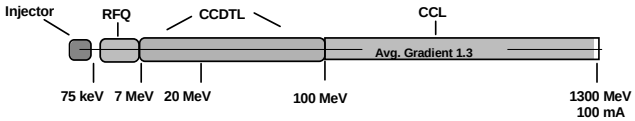

Fig. 1. Schematic layout of the APT normal conducting linac.

Post-RFQ Acceleration

Figure 2 summarizes the configuration of the accelerating scheme beyond the RFQ. The transverse focusing lattice is FODO with a constant focusing period of $8\beta\lambda$. We define the length of $4\beta\lambda$ between two consecutive electromagnetic quadrupoles (EMQ) of opposite polarity as a "segment." Between 6.7 and 8 MeV, there are only two accelerating gaps per segment. At low energy, a minimum length of $2.5\beta\lambda$ is needed for the EMQs. In the remaining length of $1.5\beta\lambda$ only one cavity containing two gaps can be placed. As β increases, we can use more gaps per cavity. Between 8 and 20 MeV, we have 3 gaps per segment provided by two drift tubes in one cavity. The structure has 4 accelerating gaps per segment between 20 to 100 MeV, which increases the packing fraction (ratio of the active accelerating length to the total length of a segment) to 0.75. The conventional CCL starts at 100 MeV. Both CCDTL and the CCL are coupled cavity structures. Hence, from beam-dynamics point of view, it is not a transition in structure. At this energy, β is large enough for six $0.5\ \beta\lambda$ coupled-cavity cells (accelerating gaps) with $1\beta\lambda$ space available for EMQs. The packing fraction remains 0.75. At 155 MeV, where we add a seventh cell to each segment, the

packing fraction increases to 0.875. The pattern continues to the final energy of 1300 MeV.

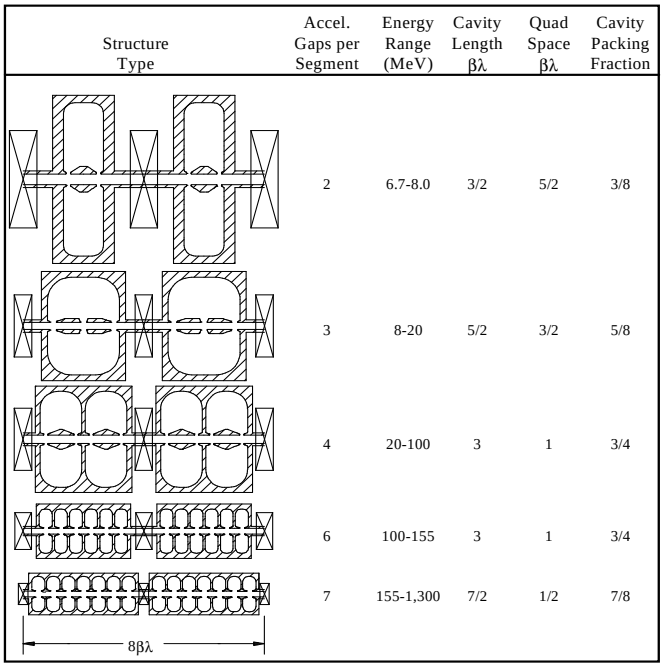

Fig. 2. Schematic for five different types of cavity configurations in the linac beyond the RFQ.

Effective shunt impedance for cavities as a function of β are calculated by the 2-D code SUPERFISH. Except for the very beginning of the coupled cavity structure (<10 MeV), we keep the real-estate shunt impedance ZT^2 above 35 MΩ/m. Consistent with this choice, we open up the bore radius as quickly as practicable. Figure 3 shows the average real estate shunt impedance as a function of energy while the variation of the bore radius along the length of the linac is shown in Fig. 8.

For power partitioning, each supermodule (chains of up to 160 coupled-accelerating cells driven in common by multiple klystrons) is fed by 4 to 6 klystrons. This concept permits the addition of an extra klystron to each supermodule i.e., operate each supermodule with 5 to 7 klystrons, thus providing redundancy in the system.

The design of the transition region involved tailoring the end of the RFQ as well as first few periods of the CCDTL. General design philosophy of this region is described in Ref. 8 while the detail is contained in Ref. 7. Following this capture section, there is a quasi-adiabatic ramp in both the synchronous phase φ_s and the field accelerating gradient E_0T. Both are initially ramped adiabatically up to 11.4 MeV. We start at $\varphi_s = -60^0$ to assure capture of the beam in the "bucket". We then ramp down $|\varphi_s|$ and ramp up E_0T adiabatically while maintaining a large ratio between the bucket and the beam-size. The structure E_0, real estate E_0, real-estate E_0T, and acceleration-rate variation as a function of energy are shown in Fig. 4. The design goal was to obtain a smooth variation in the real-estate E_0T until a predetermined value of real-estate E_0T is reached. ZT^2 values dictate the bore radius which does not vary smoothly with energy. Since transit time factor is also dependent on the radius, the structure E_0 does not show a continuous variation as seen in Fig. 4. At 155 MeV, we achieve a real-estate E_0T of 1.3 MV/m which is held constant thereafter to conserve power. The design parameters of the entire linac are given in Table 1.

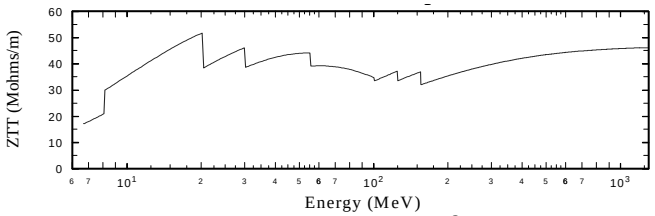

Fig. 3. Average real estate shunt impedance ZT^2 vs. energy.

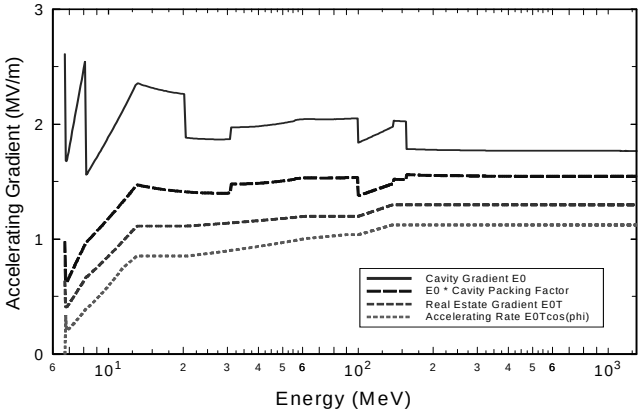

Fig. 4. Various field gradient measures vs. energy.

Table 1. Design Parameters of the Linac.

Parameter	**RFQ**	**CCDTL**	**CCL**
Energy (MeV)	0.075-6.7	6.7-99.6	99.6-1300
Frequency (MHz)	350	700	700
Beam Current (mA)	100	100	100
Aperture Radius (mm)	2.3-3.4	10.0-17.5	17.5-25.0
Cavity E_0T (MV/m)	1.38	1.095-1.574	1.574-1.485
Real Estate E_0T (MV/m)	1.38	0.410-1.180	1.180-1.300
Synchronous Phase (deg)	-90 to -60	-60 to -30	-30
Real Estate ZT^2 (MΩ/m)	-	18-33	33-47
Quad Lattice	-	FODO	FODO
Quad Length (mm)	-	30.0	30.0
Quad Gradient (T/m)	-	87.5	87.5
Trans. Emit. (π cm. mrad)$^+$	0.022	0.023	0.023
Long. Emit. (π deg. MeV)$^+$	0.214*	0.450**	0.482**
Aper. rad. / rms beam-size	-	5-13	13-26

+ emittances are rms, normalized; * @ 350 MHz; ** @700 MHz

Simulation

The computer code PARMILX [9], a modified version of PARMILA, was used to both generate and simulate the performance of the linac beyond the RFQ. An end-to-end simulation was performed with 100,000 macro-particles at the entrance to the RFQ. A 4-D waterbag distribution was assumed at the input.

Transverse phase space distributions at 1.3 GeV for full current of 105 mA are shown in Fig. 5. Beam profile plots for full current from 155 MeV to 1.3 GeV are shown in Fig. 6. No

profile oscillations indicate a good match in the transition region. Longitudinal and transverse emittances vs. energy are

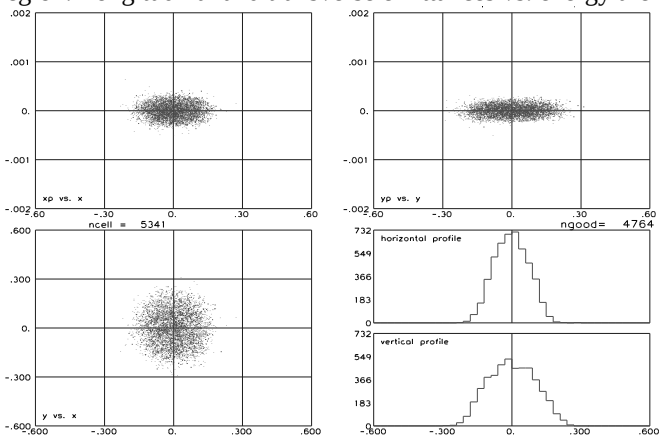

Fig. 5. Phase space distribution at 1.3 GeV for 105 mA.

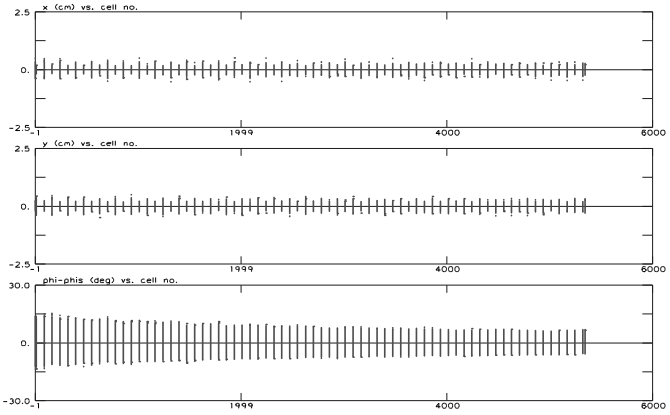

Fig. 6. Beam profile plots from 155 MeV to 1.3 GeV for 105 mA.

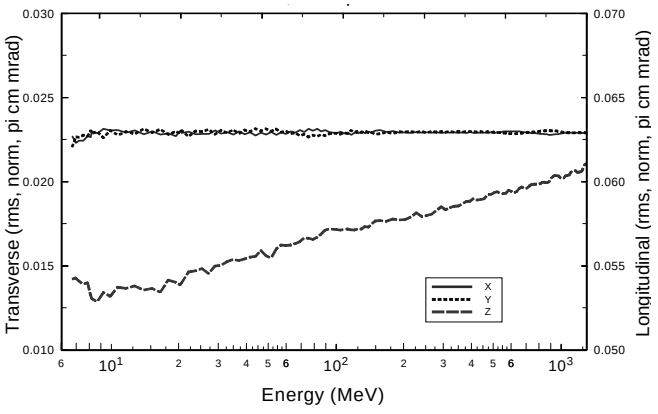

Fig. 7. Longitudinal and transverse emittance vs. energy for 105 mA.

plotted in fig. 7. There is essentially zero transverse emittance growth from 6.7 MeV to 1.3 GeV. Since the real-estate accelerating gradient E_0T is constrained to 1.3 MV/m above 155 MeV, the longitudinal focusing grows weaker. As a consequence, a longitudinal emittance growth of ~ 15 % is observed. However, this is of little concern since longitudinal beam-size is very small compared to the bucket-size and luminosity requirements are not important for this application. Figure 8 shows the relationship between beam-size (rms), aperture-size, and maximum radius of a particle as a function of energy. This particle is the outermost one in the distribution, outside the core distribution and constitutes a particle in the halo. Even at higher energies, this particle does not occupy more than ~ 25% of the bore.

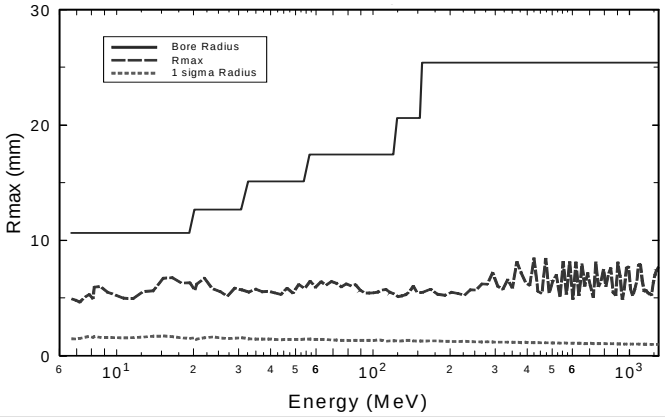

Fig. 8. Beam-size (rms), aperture-size, and maximum radius of the outermost particle vs. energy.

Conclusion

We have described the conceptual design for a high-current normal-conducting linac specifically designed to deliver a high-power proton beam on an extended target. A very high bore- to beam-size ratio was achieved at higher energies where beam-loss is of concern. Simulations show zero transverse emittance growth for the entire linac.

References

[1] J. H. Billen et al., "A New rf Structure for Intermediate-Velocity Particles," Proceedings of the 1994 Linear Accelerator Conference, Tsukuba, Japan, August 21-26, 1994.

[2] G. Lawrence et al., "Conventional and Superconducting RF Linac Design for the APT Project," this conference.

[3] Los Alamos National Laboratory APT Topical Report, LA-UR-95-1480, March, 1995.

[4] L. M. Young, "Segmented Resonantly coupled Radio Frequency Quadrupole (RFQ)," Proceedings of the 1993 Particle Accelerator Conference, Washington D.C., May17-20, 1993.

[5] "RFQ Design Codes," Los Alamos National Laboratory Document, LA-UR-96-1836, May, 1996.

[6] N. J. Diserens, Atomic Energy of Canada Limited Research Company Internal Report (unpublished), RC-1048, July, 1993.

[7] S. Nath et al., "Front-End Physics Design of APT Linac," this conference.

[8] J. H. Billen et al., "Smooth Transverse and Longitudinal Focusing in High-Intensity Ion Linacs," this conference.

[9] H. Takeda et al., "Modified PARMILA Code for New Accelerating Structure," Proceedings of the 1995 Particle Accelerator Conference and International Conference on High Energy Accelerators, Dallas, Texas, May 1-5, 1995.